5D.1 A CASE STUDY OF NEARSHORE DRAG COEFFICIENT BEHAVIOR DURING HURRICANE IKE (2008)

Brian C. Zachry[*1], Andrew B. Kennedy[2], John L. Schroeder[3], Joannes J. Westerink[2], and Chris W. Letchford[4]

[1]AIR Worldwide, Boston, MA
[2]Univeristy of Notre Dame, Notre Dame, IN
[3]Texas Tech University, Lubbock, TX
[4]Rensselaer Polytechnic Institute, Troy, NY

1. INTRODUCTION

Roughly 37 million people currently live in hurricane prone coastal regions stretching from Texas to North Carolina and a continued increase in population is inevitable. As a result, there is an urgent need for observations of surface layer quantities to improve hurricane storm surge forecasting and to define conservative wind loading provisions in the ASCE Standard in this critical region. Recently, many deep water datasets have been collected and analyzed, but there is a significant data gap in shallow water and near the coast. This void is primarily due to the low frequency of hurricane landfalls and the profound difficultly in conducting in situ measurements in extreme conditions.

Over the past decade, numerous field and laboratory experiments have examined air-sea momentum exchange in the deep ocean during moderate to strong wind conditions. The transfer of momentum from the air to the sea is typically described in terms of a 10 m drag coefficient C_D, defined as:

$$C_D = \frac{\tau_o}{\rho_a \overline{U}_{10}^2} = \frac{u_*^2}{\overline{U}_{10}^2}, \qquad (1)$$

where ρ_a is the density of air, τ_o is the surface wind stress, u_* is the friction (or shear) velocity, and U_{10} is the mean wind speed measured at the standard height of 10 m. Powell et al. (2003) and Donelan et al. (2004) found that the drag coefficient increases with increasing wind speed and reaches a limiting value of around 0.0025 at wind speeds near hurricane force. Black et al. (2007) observed a similar relationship, but with the drag coefficient saturating at a value near 0.0018 at weaker wind speeds of 22-23 m s^{-1}. The limiting nature of the drag coefficient has been attributed to the effects of spray droplets acting to limit turbulent mixing, and in short-fetch conditions, saturation is likely a result of air-flow separation from the dominant waves where the flow skips from crest to crest, sheltering the wave surface (e.g., Kudryavtsev and Makin 2007).

* *Corresponding author address*: Brian C. Zachry, AIR Worldwide, Boston, MA, 02116; email: bzachry@air-worldwide.com

Near the shore, wave interaction with the local bathymetry causes wave conditions to be markedly different from those in deep water. The nearshore region is characterized by a rapidly evolving water surface profile due to wave shoaling and breaking transformation processes. At present, nearshore wind stress is not completely known and only a few studies exist on this topic. Consequently, deep water surface drag coefficient parameterizations are commonly used for storm surge modeling and analysis. Anctil and Donelan (1996) observed higher drag over shoaling waves compared to both deep water and breaking waves in Lake Ontario, Canada. For wind speeds of around 14 m s^{-1}, they estimated the shoaling wave drag coefficient to be 0.0028, which is higher than deep water values at similar wind speeds. Data reported in Powell (2008) also suggests increased drag in the nearshore region. Based on these studies and the differences stated above, it is believed that deep water wind stress parameterizations do not allow for reliable estimation of the nearshore wind setup and are a potential culprit for the inaccurate predictions of surge.

The work presented here aims to advance our understanding of momentum exchange at the coast and in complex wave conditions. Rare measurements of hurricane winds in marine exposure were obtained using a Texas Tech University (TTU) StickNet platform during the passage of Hurricane Ike in 2008. The StickNet was inundated by surge during the peak of the storm with a predominant wind direction from across the Houston ship channel. To estimate the surge at the probe and also the wave conditions in the ship channel, a storm surge hindcast was conducted using a coupled SWAN+ADCIRC simulation. Drag coefficient behavior is determined for various record lengths and wind speeds reaching hurricane force.

2. FIELD INSTRUMENTATION AND SURGE HINDCAST

A total of 24 rapidly-deployable surface weather observing stations (termed StickNet) were deployed by the TTU Hurricane Research Team (TTUHRT) throughout Hurricane Ike's landfall region. To measure onshore winds in the eyewall, StickNet 110A was deployed in Old Fort Travis Park on the Bolivar Peninsula at 29.363708ºN and -94.759234ºW at 0120 UTC on 12 September 2008. This station was equipped with an RM Young Wind Monitor model 05103V. Wind speed and direction were measured at a height of

2.25 m with a sampling frequency of 5 Hz. For additional information on SitckNet, consult Skinner (2011).

StickNet 110A was deployed very near the water in order to measure hurricane winds in marine exposure. At its closest point and in benign conditions, the station was located about 90 m from the water at an elevation of approximately 3.71 m NAVD88. Wind flow at the probe was unobstructed in all directions with an onshore component (fetch off the water), except from 90º-110º due to air flow interference with Fort Travis (roughly 150 m from StickNet 110A). Ike had a relatively large eye at landfall with a radius of maximum wind estimated to be 74 km. The official storm center passed less than 15 km to the west of probe 110A, allowing for 'classic' hurricane eye passage time histories (see Fig. 1). Marine winds were measured in Ike's southern eyewall, as the wind direction shifted from around 30º-60º to 190º-230º with a fetch across the Houston ship channel (approximately 3 km wide). The wind measurements and ultimately the derived surface layer quantities are representative of the wave roughness in the channel.

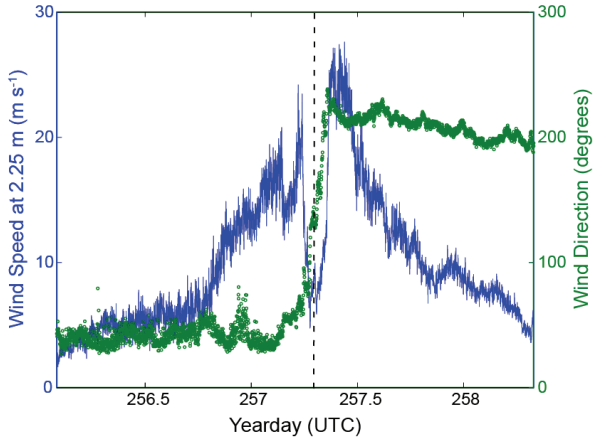

FIG. 1. Raw 1-min wind speed and wind direction time records (at 2.25 m) obtained from StickNet 110A during the passage of Hurricane Ike. Landfall is denoted by the vertical dashed line.

Unlike the open ocean where NOAA buoys and rapid-response gauges (e.g., Kennedy et al. 2010) are quite ubiquitous, wave conditions in the ship channel were not measured and must be simulated using numerical models. To obtain a better understanding of the wave conditions in the ship channel and the inundation at StickNet 110A, a wave and surge hindcast was conducted using a coupled wave and circulation approach via Simulating Waves Nearshore (SWAN) and the Advanced Circulation Model (ADCIRC), denoted SWAN+ADCIRC (Dietrich et al. 2011). The hindcast was simulated on the SL18+TX grid, which is an unstructured, finite-element mesh that contains 9,228,245 nodes and 18,300,169 elements. The simulation was conducted for a total of 39 days, which included Hurricanes Gustav and Ike and a spin up time of 18 days to allow the tidal signal to be replicated with constituents K1, O1, M2, S2, N2, K2, Q1, and P1. The surface stresses were forced by an Ocean Weather Inc. representation of the wind field (Powell et al. 1996, Powell et al. 1998, Powell et al. 2010) and a drag coefficient formulation following Garratt (1977) with the radial dependence of Powell et al. (2008). Initial water levels were raised to 0.280 m to adjust for seasonal expansion and the vertical datum adjustment, and the river flux in the Mississippi was set to 12,318 m^3/s. Wave and water level properties were saved at hourly intervals for the analysis.

The bathymetry in the ship channel is not representative of a typical beach shoreline, where waves propagate towards the shore from oceanic deep water. In the vicinity of Fort Travis (termed inner bar channel by the US Army Corps of Engineers) the channel is approximately 14 m deep. Near the edges, the channel is shallow (similar to any coast), but drops off quickly with a slope of 2.5:1. In the center of the channel (29.350335ºN,-94.771247ºW), the SWAN+ADCIRC simulated waves were indicative of a fetch-limited condition with maximum significant wave heights reaching 1.5 m and peak periods of approximately 4 s, as shown in Fig. 2. A maximum water level of 4.17 m NAVD88 was simulated in the channel. At the StickNet, the water level reached a maximum height of 4.3 m NAVD88 during the peak of the storm, and remained inundated for approximately 5 hours (from 06Z 13 Aug to 10Z 13 Aug). Using the elevation of the grid cell inherent in SWAN+ADCIRC, a maximum water depth of 0.6 m was hindcast, which is in agreement with a high water mark of approximately 0.6 m measured on the StickNet during retrieval.

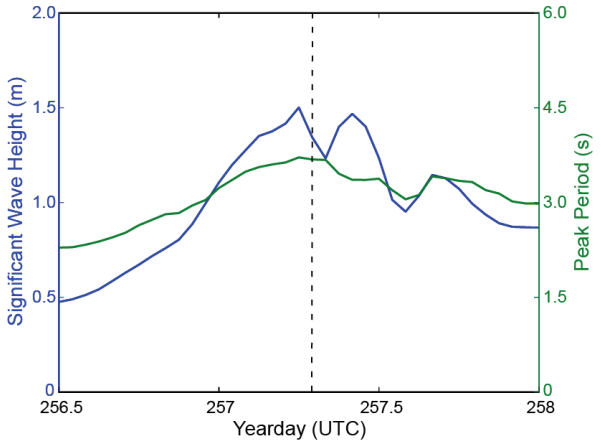

FIG. 2. SWAN+ADCIRC hindcast of significant wave height and peak period in the center of the Houston ship channel during the passage of Hurricane Ike.

3. METHODOLOGY

3.1 *StickNet 110A Wind Measurements*

Based on estimates of boundary layer growth (e.g., Simiu and Scanlan 1986; Homles 2001), StickNet 110A

measured marine-type winds with flow across the ship channel. With the station being rough 90 m from the water, the boundary layer was representative of marine roughness (or at minimum in a transitional phase) depending on the assumptions of the roughness length and the theoretical relationship employed. Individual power spectral densities (PSD) were computed for a 1-hour data segment during landfall of Ike's southern eyewall for when the wind flow was across the channel. For this time period, the 2-min mean wind speed averaged 26.8 m s^{-1}. In each PSD, the longitudinal wind record contained more low frequency energy and significantly less high frequency energy than predicted by the empirical relations, as shown in Fig. 3. The increased low frequency energy, which has been observed in other studies (e.g., Schroeder et al. 1998), is attributed to the hurricane environment. The lack of high frequency energy is a result of the poor response characteristics of the R. M. Young Wind Monitor, and attenuation is evident at the high frequency end of the inertial subrange, where the PSD do not follow the $f^{(-2/3)}$ slope.

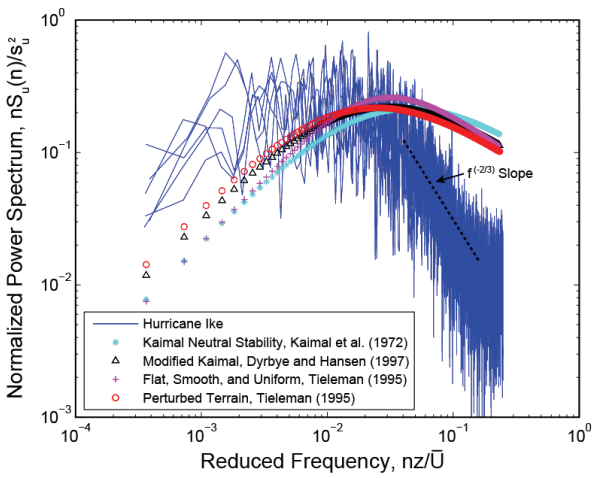

FIG. 3. Normalized longitudinal power spectral density for six individual 10-min segments during landfall of Hurricane Ike's southern eyewall, during which the wind flow was across the Houston ship channel.

Since the StickNet only collects single-level wind data, the turbulence intensity (TI) method (e.g., Barthelmie et al. 1993) was utilized to estimate the roughness length. Generally speaking, TI characterizes the intensity of gusts in the flow and is defined as the ratio of the standard deviation of fluctuating wind to the mean wind speed. Using TI, the roughness length and the drag coefficient are computed as follows:

$$z_o = z_a \exp\left[-\frac{1}{TI}\right], \quad C_D = k^2\left[\ln\left(\frac{z_a}{z_o}\right)\right]^{-2}, \quad (2)$$

where z_a = 2.25 m is the anemometer height and k = 0.4 is the von Kármán constant. This method assumes a logarithmic wind profile and that the ratio of the standard deviation to the friction velocity is 2.5, which is valid in smooth terrain for z_o < 0.1 m (e.g., Counihan 1975). The inherent variation in TI with height is accounted for in the assumptions used in its derivation. Along with other wind statistics, TI varies based on averaging time. To determine where TI stabilizes, the wind speed record was windowed into various averaging times and mean, maximum, and minimum values of TI were computed (see Fig. 4). An averaging time of 2-min was utilized for this work, as this window length captures variations in the smaller scales of motion, which are driven by surface roughness. Also, TI becomes fairly stable by 2-min with only a modest increase of 6.0% from 2- to 10-min.

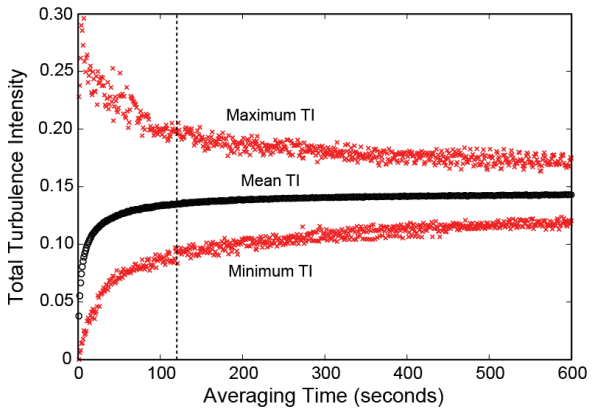

FIG. 4. Dependency of the total turbulence intensity (TI) on averaging time. A 2-min averaging time (used in this study) is denoted by the vertical dashed line.

TI is sensitive to nonstationarities (e.g., mean and variance) present in the wind speed record, as these moments are used to calculate TI. Nonstationarities lead to anomalous TI values, which directly affect the estimation of z_o and ultimately C_D. The rationale is to test for the presence of a trend (i.e., a changing mean or variance value) due to a source of nonstationarity in the signal. To remove nonstationary segments from the wind speed record, the modified reverse arrangement test was conducted at a significance level of α = 0.01 following Bendat and Piersol (1986). Wind speed data segments with stationarity with respect to both the mean and variance were used in the analysis. The majority of nonstationary segments were due to trends in the first moment.

3.2 SWAN+ADCIRC Wave and Surge Hindcast

The SWAN+ADCIRC simulation of Hurricane Ike provides a means to characterize the upstream flow and also the water level at the StickNet. As mentioned in Section 2, the wave conditions in the ship channel are indicative of a fetch-limited condition. It should be noted that the hourly output from SWAN+ADCIRC does not completely capture the complex wave conditions in the ship channel. Conceptually, there were two wave fields

interacting: (1) swell that propagated into the ship channel from the Gulf of Mexico and (2) the local wind-driven waves (which are captured in the hourly significant wave height), both of which contribute to the underling wave roughness in this complex environment. In addition to this highly complex interaction among the wave fields, local changes in bathymetry, wave interaction with breakwaters, refraction and diffraction, and strong currents complicate the situation.

The developmental stage of the sea relative to the current state of wind forcing is often described by the so-called 'wave age' parameter, which can be expressed as the wave phase speed divided by the wind speed, c_p/U_{10}. For growing seas, or seas in which the wind has just begun to act on the ocean surface to develop wind waves or the fetch is limited, the wave age parameter is small (less than 0.5), as the wind speed is much faster than the wave celerity (e.g., Sjöblom and Smedman 2002). During landfall of Ike's southern eyewall, the wave age parameter remained relatively stable, was estimated to be as low as 0.18, and did not surpass 0.4 based on linear wave theory (e.g., Dean and Dalrymple 1991). This value is much lower than hurricane waves in the open ocean where wave phase speeds are much faster.

Since the StickNet was inundated by surge during the storm (see Fig. 5), an additional scaling factor is necessary to determine the wind characteristics. This is because the water rise acts to change the theoretical height of the anemometer relative to the ground/water surface. These height changes affect z_o estimates via the TI method and the wind speed translation up to 10 m. Any depth of water lowers the anemometer height, resulting in lower z_o, faster 10 m wind speeds, and thus lower 10 m drags. Where indicated below, this scaling was taken into account using the time series of local water level hindcast by SWAN+ADCIRC.

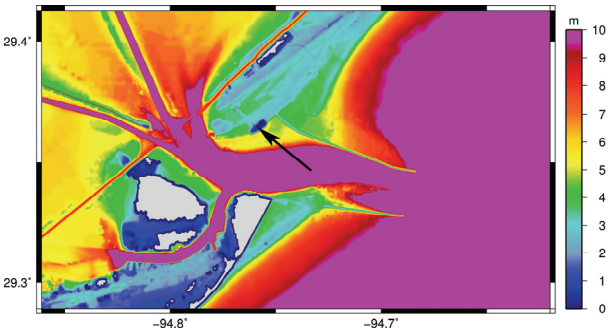

FIG. 5. Hindcast water depth (i.e., water level above local ground elevation) by a SWAN+ADCIRC simulation using the SL18+TX finite element mesh in the Houston, TX area. The black arrow points to the approximate location of StickNet 110A in Fort Travis on the Bolivar Peninsula.

4. ANALYSIS AND DISCUSSION

The primary interest of this work is to determine drag coefficient behavior with wind speed. It is customary to report the drag coefficient (and other parameters) to the standard 10 m height. Mean wind speed data obtained at 2.25 m were referenced to 10 m using the neutral stability log-law. In the surface layer, shear stress is assumed to be constant with height (e.g., Stull 1988), and hence the 2.25 m drag coefficient can be translated to the standard 10 m height using:

$$C_{D(10)} = C_{D(2.25)}\left[\frac{\overline{U}_{2.25}}{\overline{U}_{10}}\right]^2 . \qquad (3)$$

The drag coefficient was analyzed for three different time durations (see Fig. 6). Over these time periods, the wind direction remained relatively stable with a fetch across the ship channel. Durations of 12 and 22 hours were used to determine the dependence of the drag coefficient with wind speed. The longer record shows the difference at lower wind speeds, as the highest wind speeds occurred in the first few hours and the slowest near the end of the record. Based on the hindcast, the StickNet was inundated by surge for only 1.03 hours of the analysis length. This duration is relatively short and only surface layer quantities for this record were determined.

The standard way to assess C_D versus U_{10} is to partition the wind speed data (and corresponding C_D values) into bins with equal ranges. Binning is advantageous, as the trend in C_D with wind speed can be determined. Six wind speed bins of 5 m s^{-1} were chosen ranging from 5-10 m s^{-1} to 30-35 m s^{-1}. Although the number of bins employed is somewhat arbitrary, there must be a sufficient number of data points in each bin to be a representative sample. With a limited number of 2-min onshore wind regime data segments acquired during Hurricane Ike (especially for the strongest winds), it is assumed that if the number of data points in each bin is greater than 10, a reasonable sample size has been achieved.

Statistics for the different wind record durations binned into six wind speed groups are Table 1. Mean 2-min wind speeds are nearly centered in each of their respective bins, except for the 20-25 and 25-30 m s^{-1} bins. Ideally, one would want the wind speeds in each bin to be centered; however, due to the relatively few number of data points in these bins, this is rather difficult to achieve. Wind directions are very similar for the strongest wind speeds. For slower speeds the winds have a greater southerly component. This is a result of the winds backing as the hurricane moved north of the region late in the record (where the weaker winds were observed). Regardless, mean wind directions for each bin are within 20º (with relatively small standard deviations), showing that a very similar fetch existed throughout the records.

TABLE 1. Drag coefficient referenced to 10 m for different wind speed bins and record lengths. Values are also reported with and without the correction (denoted 'Corrected') to the wind speeds via SWAN+ADCIRC hindcast water levels. Observed wind speeds at 2.25 m were translated to 10 m using the neutral stability log-law.

		U_{10} Bins (m s^{-1})					
Record	**Statistic**	**5–10**	**10–15**	**15–20**	**20–25**	**25–30**	**30–35**
12 Hour	Number of 2-min Segments	13	108	90	33	49	18
	Mean Wind Speed	9.54	12.9	17.4	21.8	27.9	31.0
	St. Dev. Wind Speed	0.326	1.50	1.50	1.33	1.41	0.812
	Mean Wind Direction	211	213	219	214	217	220
	St. Dev. Wind Direction	1.56	3.60	4.70	2.06	5.56	6.67
	Mean Roughness Length × 10^3	0.760	1.68	1.77	2.14	2.37	2.11
	St. Dev. Roughness Length × 10^3	0.710	1.66	1.25	1.63	1.86	1.37
	Mean Drag Coefficient × 10^3	1.67	1.99	2.07	2.16	2.22	2.16
	St. Dev. Drag Coefficient × 10^3	0.362	0.434	0.343	0.365	0.370	0.353
12 Hour, Corrected	Number of 2-min Segments	13	108	90	33	42	25
	Mean Wind Speed	9.54	12.9	17.4	21.8	28.0	31.2
	St. Dev. Wind Speed	0.326	1.50	1.50	1.33	1.47	0.971
	Mean Wind Direction	211	213	219	214	216	220
	St. Dev. Wind Direction	1.56	3.60	4.70	2.06	5.52	6.10
	Mean Roughness Length × 10^3	0.760	1.68	1.77	2.14	1.87	2.23
	St. Dev. Roughness Length × 10^3	0.710	1.66	1.25	1.63	1.29	1.85
	Mean Drag Coefficient × 10^3	1.67	1.99	2.07	2.16	2.11	2.17
	St. Dev. Drag Coefficient × 10^3	0.362	0.434	0.343	0.365	0.310	0.394
22 Hour	Number of 2-min Segments	192	196	90	33	49	18
	Mean Wind Speed	8.55	12.1	17.4	21.8	27.9	31.0
	St. Dev. Wind Speed	1.07	1.50	1.50	1.33	1.41	0.812
	Mean Wind Direction	200	210	219	214	217	220
	St. Dev. Wind Direction	4.84	4.64	4.70	2.06	5.56	6.67
	Mean Roughness Length × 10^3	1.32	1.68	1.77	2.14	2.37	2.11
	St. Dev. Roughness Length × 10^3	1.26	1.65	1.25	1.63	1.86	1.37
	Mean Drag Coefficient × 10^3	1.89	1.99	2.07	2.16	2.22	2.16
	St. Dev. Drag Coefficient × 10^3	0.387	0.431	0.343	0.365	0.370	0.353
22 Hour, Corrected	Number of 2-min Segments	192	196	90	33	42	25
	Mean Wind Speed	8.55	12.1	17.4	21.8	28.0	31.2
	St. Dev. Wind Speed	1.07	1.50	1.50	1.33	1.47	0.971
	Mean Wind Direction	200	210	219	214	216	220
	St. Dev. Wind Direction	4.84	4.64	4.70	2.06	5.52	6.10
	Mean Roughness Length × 10^3	1.32	1.68	1.77	2.14	1.87	2.23
	St. Dev. Roughness Length × 10^3	1.26	1.65	1.25	1.63	1.29	1.85
	Mean Drag Coefficient × 10^3	1.89	1.99	2.07	2.16	2.11	2.17
	St. Dev. Drag Coefficient × 10^3	0.387	0.431	0.343	0.365	0.310	0.394
1.03 Hour	Number of 2-min Segments	-	-	-	-	15	12
	Mean Wind Speed	-	-	-	-	28.2	31.1
	St. Dev. Wind Speed	-	-	-	-	1.08	0.777
	Mean Wind Direction	-	-	-	-	223	225
	St. Dev. Wind Direction	-	-	-	-	3.03	4.02
	Mean Roughness Length × 10^3	-	-	-	-	2.72	2.19
	St. Dev. Roughness Length × 10^3	-	-	-	-	1.82	1.31
	Mean Drag Coefficient × 10^3	-	-	-	-	2.31	2.20
	St. Dev. Drag Coefficient × 10^3	-	-	-	-	0.359	0.307
1.03 Hour, Corrected	Number of 2-min Segments	-	-	-	-	15	12
	Mean Wind Speed	-	-	-	-	28.8	31.6
	St. Dev. Wind Speed	-	-	-	-	1.07	1.019
	Mean Wind Direction	-	-	-	-	222	225
	St. Dev. Wind Direction	-	-	-	-	3.09	3.49
	Mean Roughness Length × 10^3	-	-	-	-	2.03	1.97
	St. Dev. Roughness Length × 10^3	-	-	-	-	1.51	1.06
	Mean Drag Coefficient × 10^3	-	-	-	-	2.14	2.15
	St. Dev. Drag Coefficient × 10^3	-	-	-	-	0.344	0.283

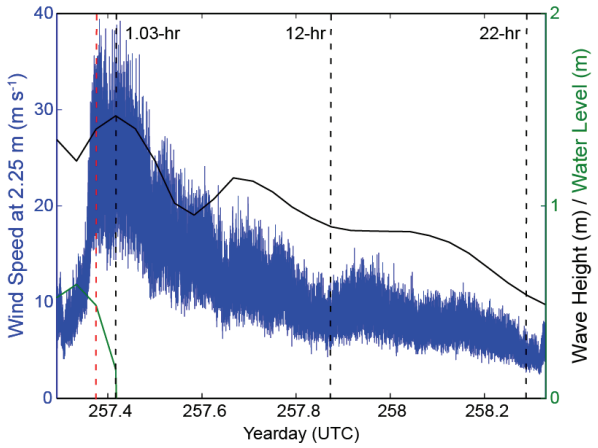

FIG. 6. Time series of wind speed (blue line), water level (green line), and significant wave height (black line) used in the analysis. The vertical red dashed line corresponds to the start of the record used in the analysis and the black vertical dashed lines correspond to analysis lengths of 1.03 hours (during which the StickNet platform was inundated by surge based on the SWAN+ADCIRC hindcast), 12 hours, and 22 hours.

Binned drag coefficients are plotted against wind speed in Fig. 7. For the 12 and 24 hour durations without correction for water levels at the StickNet, the drag coefficient increases with wind speed initially, reaches a limiting value of 0.0022 at a wind speed near 28 m s^{-1}, and decreases for wind speeds above 28 m s^{-1}. Compared to the 12 hour record, the drag coefficient is higher at lower wind speeds for the 22 hour record. This could be a result of sample size or increased land exposure and hence roughness at the end of the record as the water receded from the Bolívar and the water level in the ship channel subsided. When the correction for water level is taken account, only the highest two winds speeds bins are affected and thus the result as slower wind speeds are the same. In the 30-35 m s^{-1} wind speed bin, the drag coefficient increase minimally from the non-corrected analysis and in the 25-30 m s^{-1} bin values decrease significantly. Regardless, a limiting value has been reached, but data at higher wind speeds would be necessary to confirm any trends.

Drag coefficients in this complex environment are compared with other studies in Fig. 8. Three well-known deep water studies were utilized for the comparison (Powell et al. 2003; Donelan et al. 2004; Black et al. 2007), as well as shallow water drag coefficients reported in Powell (2008). The drag coefficient values in Fig. 8 for Powell et al. (2003) are an average of their four layers and for Donelan et al. (2004) are the laboratory values determined using the momentum budget method. The present work is consistent with the deep water studies in that C_D reaches a limiting value and either decreases or remains relatively constant for higher wind speeds. The nearshore (or coastal) limiting drag coefficient found during Hurricane Ike is similar in magnitude to deep water values, in which the former falls within the range of deep water limiting drag coefficients. In regards to the wind speed of C_D saturation, the coastal drag coefficient reached a limiting value at slower wind speeds than Powell et al. (2003) and Donelan et al. (2004) and at faster wind speeds than Black et al. (2007). There is not sufficient data to compare the limiting values to the nearshore values presented in Powell et al. (2008).

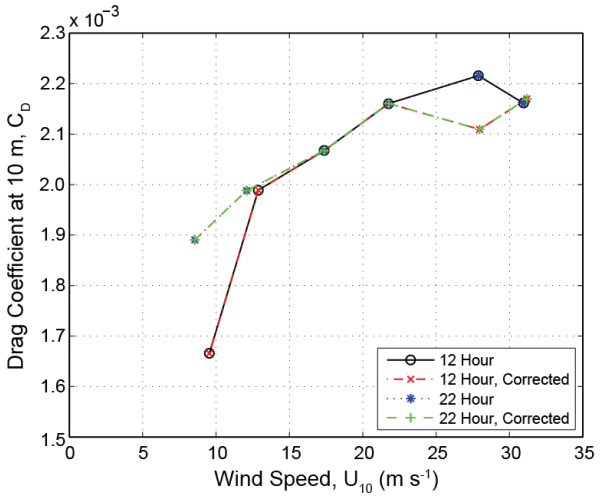

FIG. 7. Drag coefficient dependence on wind speed for various record lengths and for with and without correction (denoted 'Corrected') to the wind speeds based on SWAN+ADCIRC hindcast water levels at the StickNet platform.

Examination of Fig. 8 also reveals that coastal drags are significantly higher for low to moderate wind speeds of less than 25 m s^{-1} regardless of record length. Powell et al. (2003) and Powell (2008) deep and shallow water data decreased rapidly for wind speeds below hurricane force. Crudely extrapolating their results to slower winds (e.g., 10 m s^{-1}) the drag coefficient would be markedly less than those obtained here during Hurricane Ike. Laboratory observations from Donelan et al. (2004) also indicate lower drags for lighter winds and that the trend in C_D with increasing wind speed is much steeper than the present study. This result is likely a consequence of the fetch-limited and complex wave conditions in the Houston ship channel generating a 'rough' (wave) surface even under light wind conditions.

5. SUMMARY AND CONCLUDING REMARKS

Field observations of coastal wind measurements were obtained during the passage of Hurricane Ike. StickNet 110A on the Bolivar Peninsula measured wind data at 2.25 m with the mean flow coming across the Houston ship channel. Wave conditions in the channel were extremely complex. Strong cross-channel winds generated fetch limited waves across the 3 km wide channel and swell waves coming into the ship channel from the ocean and strong currents complicated the situation. The surface layer quantities presented are

representative of the wave roughness in the waterway. Results obtained in the study provide the following conclusions.

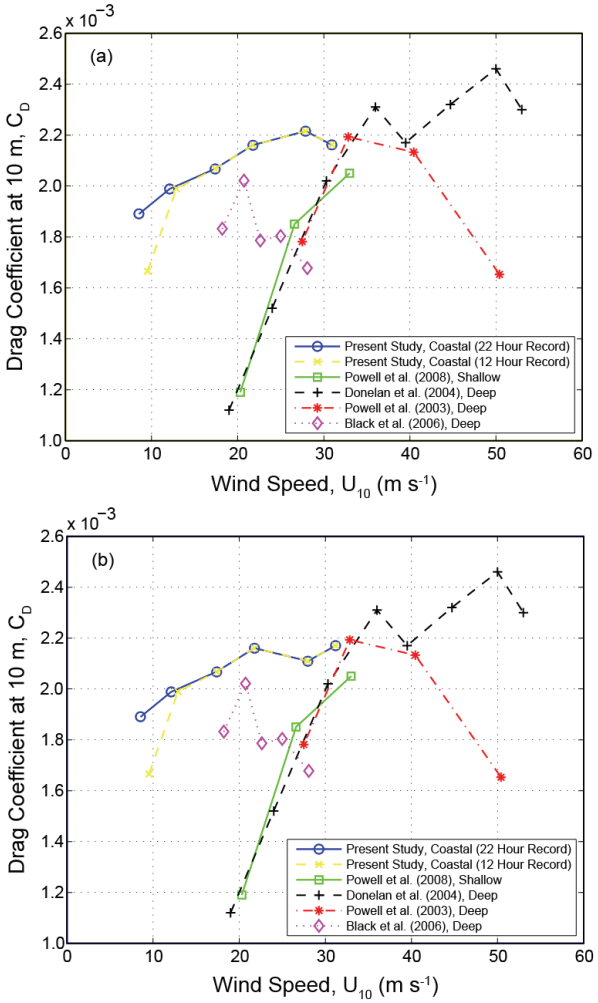

FIG. 8. Drag coefficient dependence on wind speed for this study: (a) wind speeds not corrected for water level and (b) wind speeds corrected for water level at the StickNet via SWAN+ADCIRC hindcast. Results are compared with shallow water values from Powell et al. (2008), open ocean measurements from Powell et al. (2003) and Black et al. (2007), and in simulated extreme wind in the laboratory from Donelan et al. (2004). For Powell et al. (2003) the values are an average of the four layers.

Observed drag coefficient behavior is similar to that found in deep water, where C_D increased with wind speed, reaches a limiting value, and decreases thereafter. Aerodynamic drag increased with wind speed until around 28 m s^{-1} where a limiting value of 0.0022 was reached. When wind speeds are corrected based on the SWAN+ADCIRC hindcast water levels at the StickNet, the drag coefficient levels off at slower wind speeds of 22 m s^{-1}. This provides evidence that the limiting C_D value at this location is on the order of deep water values. This may also be the case in other regions with complex bathymetry and coastal formations that interfere with the local waves, fetch limited conditions, or in regions with a wide shallow continental shelf (where the largest waves are well offshore). Saturation of C_D is likely a result of sea spray and skimming flow as the waves are fetch-limited and very steep. Higher wind speed data are needed to verify if the drag coefficient decreases with wind speeds above than hurricane force.

A significant difference between deep and shallow water drag coefficients exists at slower wind speeds. Drag coefficient values at slower wind speeds are much greater than deep water values (e.g. Powell et al. 2003) or those found in the laboratory (Donelan et al. 2004). This result could be a consequence of the complex wave conditions in the channel creating a 'rougher than normal' surface under light to moderate winds. Based on this analysis, storm surge models using a deep water wind speed dependent drag coefficient may be slightly underestimating hurricane storm surge, and additional forcing parameterizations are needed in such complex roughness situations.

Lastly, structures built on the hurricane prone coast are currently being designed to withstand wind loads specified by Exposure C. Data obtained during Hurricane Ike suggest that this region is smoother than that prescribed by ASCE 7-10. Surface roughness values (Table 1) are an order of magnitude smaller than open terrain (z_o = 30 mm), and are within the range of Exposure D (1 < z_o < 5 mm). These findings suggest that nearshore roughness is less than that prescribed by ASCE in hurricane regions, indicating that current design wind speeds may be underestimated.

6. ACKNOWLEDGEMENTS

Funding support for the lead author was provided by the National Science Foundation Interdisciplinary Graduate Research and Training (IGERT) program under Grant No. 0221688 and Texas Tech University. The authors want to acknowledge the Texas Tech Hurricane Research Team for collecting invaluable data during Hurricane Ike and the team of Joannes Westerink, in particular Mark Hope, at Notre Dame for providing the SWAN+ADCIRC hindcast.

7. REFERENCES

Anctil, F. and M. A. Donelan, 1996: Air-water momentum flux observations over shoaling waves. *J. Phys. Oceanogr.*, **26**, 1344–1353.

Barthelmie, R. J., J. P. Palutikof, and T. D. Davies, 1993: Estimation of sector roughness lengths and the effect on prediction of the vertical wind speed profile. *Boundary-Layer Meteor.*, **66**, 19–47.

Bendat, J. S. and A. G. Piersol, 1986: *Random data: analysis and measurement procedures*. John Wiley & Sons, New York, 556 pp.

Black, P. G. and Coauthors, 2007: Air-sea exchange in hurricanes: Synthesis of observations from the coupled boundary layer air-sea transfer experiment. *Bull. Amer. Meteor. Soc.*, **88**, 357–384.

Counihan, J., 1975: Adiabatic atmospheric boundary layers – review and analysis of data from period 1880-1972. *Atmos. Environ.,* **9**, 871–905.

Dean, R. G. and R. A. Dalrymple, 1991: *Water wave mechanics for engineers and scientists*. World Scientific Press, Toh Tuck Link, Singapore, 353 pp.

Dietrich, J. C. and Coauthors, 2011: Modeling hurricane waves and storm surge using integrally-coupled, scalable computations. *Coast. Eng.*, **58**, 45–65.

Donelan, M. A., F. W. Dobson, S. D. Smith, and R. J. Anderson, 1993: On the dependence of sea surface roughness on wave development. *J. Phys. Oceanogr.*, **23**, 2143–2149.

——, B. K. Haus, N. Ruel, W. J. Stianssnie, H. C. Graber, O. B. Brown, and E. S. Saltzman, 2004: On the limiting aerodynamic roughness of the ocean in very strong winds. *Geophys. Res. Lett.*, **31**, L18306.

Garratt, J. R., 1977: Review of drag coefficients over oceans and continents. *Mon. Wea. Rev*., **105**, 915–929.

Holmes, J. D., 2001: *Wind Loading of Structures*. Spon Press, London, 1–94 pp.

Kennedy, A. B., U. Gravois, B. Zachry, R. Luettich, T. Whipple, R. Weaver, J. Reynolds-Fleming, Q. Chen, and R. Avissar, 2010: Rapidly installed temporary gauging for waves and surge, and application to Hurricane Gustav. *Cont. Shelf Res*., **30**, 1743–1752.

Kudryavtsev, V. N., 2007: Aerodynamic roughness of the sea surface at high winds. *Bound. Layer Meteor.*, **125**, 289–303.

Powell, M. D., 2008: *High wind drag coefficient and sea surface roughness in shallow water*. Final report to the joint hurricane testbed.

——, S. Houston, and T. Reinhold, 1996: Hurricane Andrew's landfall in South Florida. Part I: Standardizing measurements for documentation of surface wind fields. *Wea. Forecasting*., **11**, 304–328.

——, L. Amat, and N. Morrisseau-Leroy, 1998: The HRD real-time hurricane wind analysis system. *J. Wind Eng. Ind. Aerodyn*., **77–78**, 53–64.

——, P. J. Vickery, and T. A. Reinhold, 2003: Reduced drag coefficient for high wind speeds in tropical cyclones. *Nature*, **422**, 279–283.

——, and Coauthors, 2010: Reconstruction of Hurricane Katrina's wind fields for storm surge and wave hindcasting. Ocean Eng., **37**, 26–36.

Schroeder, J. L., D. A. Smith, and R. E. Peterson, 1998: Variation of turbulence intensities and integral scales during the passage of a hurricane. *J. Wind Eng. Ind. Aerodyn*., **422**, 65–72.

Simiu, E. and R. H. Scanlan, 1986: *Wind effects on structures*. John Wiley & Sons, New York, 2nd ed., 589 pp.

Sjöblom, A. and A. Smedman, 2002: The turbulent kinetic energy budget in the marine atmospheric surface layer. *J. Geophys. Res.*, **107**, 3142.

Skinner, P., 2011: *Observations of the surface boundary structure within supercell thunderstorms*. Masters thesis, Texas Tech University, Lubbock, TX.

Stull, R.B., 1988: *An Introduction to Boundary Layer Meteorology*. Kluwer Academic Publishers, Dordrecht/Boston/London, 680 pp.

U.S. Census Bureau. Facts for features: 2011 Hurricane Season Begins. Retrieved February, 2012, from http://www.census.gov/newsroom/releases/archives/facts_for_features_special_editions/cb11-ff12.html.